

Highly labile cationic tris-acetonitrile complexes, [Tp^RM(NCMe)₃]OTf (M = Ni, Co; Tp^R: hydrotrispyrazolylborato, R = Ph, Me and iPr₂): versatile precursors for Tp^R-containing nickel and cobalt complexes †

Kazuhiro Uehara, Shiro Hikichi ‡ and Munetaka Akita *

Chemical Resources Laboratory, Tokyo Institute of Technology, 4259 Nagatsuta, Midori-ku, Yokohama 226-8503, Japan

Received 5th April 2002, Accepted 18th July 2002

First published as an Advance Article on the web 28th August 2002

The cationic tris-MeCN adducts of Tp^RM fragments, [Tp^RM(NCMe)₃]OTf [Tp^R = hydrotrispyrazolylborato, R = 3-Ph-5-Me (**1**), 3,5-iPr₂ (**1'**); M = Ni, Co], were prepared by chloride abstraction from the corresponding chloro complexes, Tp^RM-Cl (**2**), with AgOTf in acetonitrile. The MeCN ligands in **1** and **1'** are labile enough to be readily converted to a variety of adducts, [Tp^RM(L)_m]OTf, via treatment with N- and P-donors [NC(CH₂)₂CN, *p*-NCC₆H₄CN, pyridine, *o*-bipy, *p*-bipy, Ph₂P(CH₂)_mPPh₂ (*m* = 2, 3)].

Introduction

The family of hydrotris(pyrazolyl)borates (Tp^R) are versatile ancillary ligands in inorganic and organometallic studies of transition metal complexes as well as main group metal compounds¹ and we have been carrying out synthetic studies based on the Tp^RM systems ranging from the bioinorganic study of dioxygen complexes to the coordinatively unsaturated organometallic systems.² The nucleophilic displacement reaction of halo complexes, Tp^RM-X, is a useful synthetic method for derivative chemistry but the halo complexes are not always reactive enough to interact with such a weak, soft nucleophile as [Co(CO)₄]⁻, as we encountered in the synthesis of the heterodinuclear xenophilic complexes.^{2e} In such cases the Tp^RM fragment should be activated toward a nucleophile in some way. Herein we wish to describe the synthesis of labile cationic MeCN-coordinated nickel and cobalt complexes containing hydrotris(pyrazolyl)borato ligands (Tp^R), [Tp^RM(NCMe)₃]⁺ [Tp^R = Tp^{Ph,Me} (**1**), Tp^{iPr₂} (**1'**); OTf salts],³ which turn out to be useful precursors for a variety of derivatives. Details of the results obtained will be described with emphasis on the Tp^{Ph,Me} systems.

Results and discussion

Chloro complexes with the Tp^{Ph,Me} ligand, Tp^{Ph,Me}M-Cl (**2**), were readily prepared by a procedure similar to that already reported for **2'**,^{2b} *i.e.* treatment of the appropriate MCl₂·6H₂O with KTP^{Ph,Me} (Scheme 1). The virtually tetrahedral structures of **2** with the κ³-Tp^{Ph,Me} ligand were confirmed by the B-H vibration around 2545 cm⁻¹^{2c} and X-ray crystallography (see Fig. 1 and Table 1).^{4,5} When compared with the Tp^{iPr₂} derivatives **2'**^{2d} the structures of **2**^{Ni,Co} are slightly deviated from a C₃ structure as compared in Table 1. The four-coordinate Tp^{Ph,Me}-M-X-type complexes can adopt a C₃ structure when the three phenyl rings are arranged in a propeller-like conformation,⁷ but

Table 1 Selected structural parameters for Tp^RM-Cl **2** and **2'**^a

Complexes	2 ^{Ni}	2 ^{Co}	2' ^{Ni} ^b
M-Cl1	2.153(2)	2.2004(9)	2.172(2)
M-N11	1.982(5)	2.045(3)	1.975(3)
M-N12	1.981(5)	2.029(3)	1.978(4)
M-N31	2.001(5)	2.027(3)	1.965(4)
N11-M-Cl1	118.8(1)	120.98(8)	126.2(1)
N21-M-Cl1	130.7(2)	119.90(7)	123.5(1)
N31-M-Cl1	121.5(1)	124.97(8)	122.8(1)
N11-M-N21	90.0(2)	96.4(1)	92.5(1)
N11-M-N31	95.6(2)	97.3(1)	90.1(1)
N21-M-N31	91.3(2)	89.8(1)	92.0(2)
B···M-Cl	176.87(8)	172.2(2)	179.1(1)

^a Bond lengths in Å and bond angles in deg. ^b Ref. 2d.

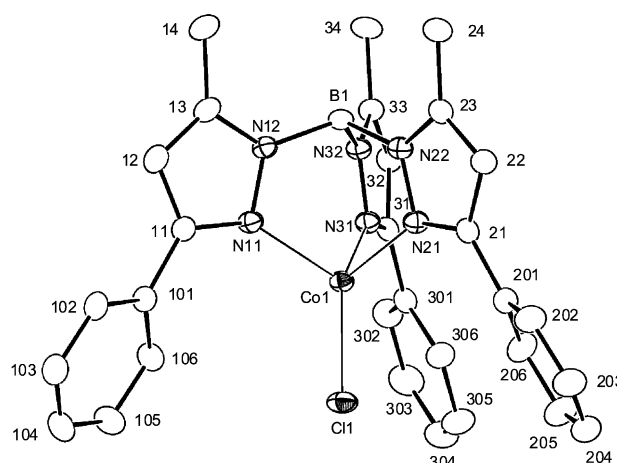
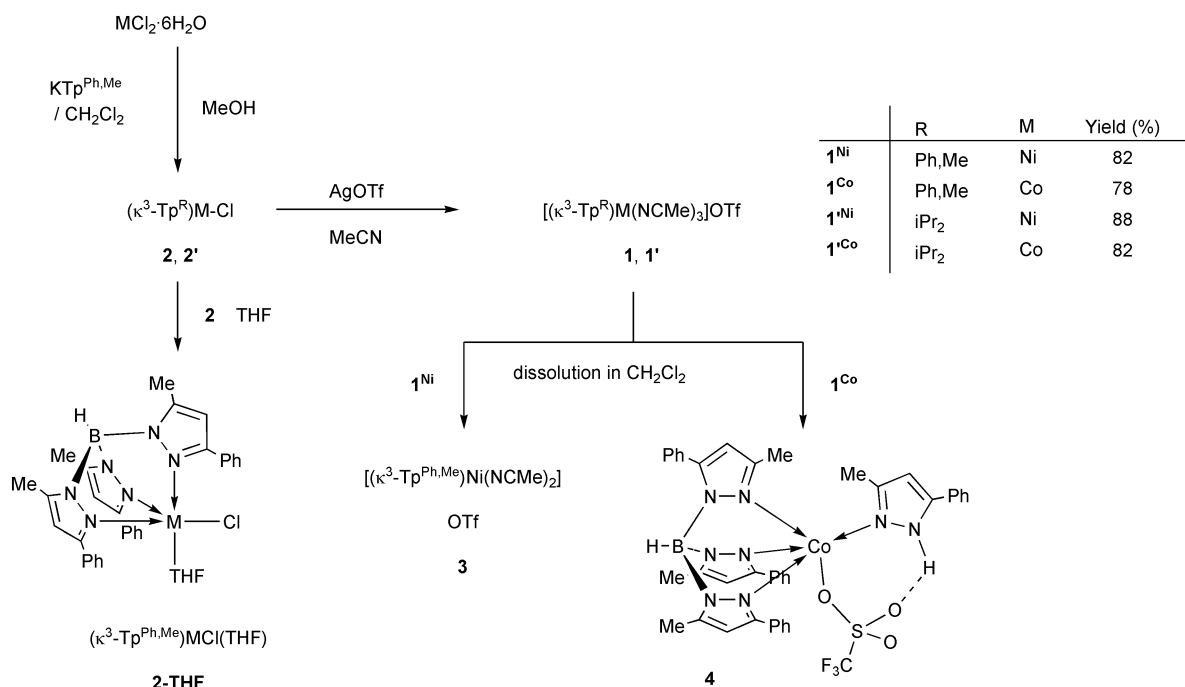


Fig. 1 Molecular structure of **2**^{Ni} showing 30% thermal ellipsoids. Labels without atom names are for carbon atoms.

such a symmetrical structure was not observed for **2**. For example, the distribution of the N-M-Cl angles for the Tp^{Ph,Me} complex **2**^{Ni} (118.8–130.7°; difference = 11.9°) is substantially larger than that of the Tp^{iPr₂} complex **2'**^{Ni} (122.8–126.2°:

† Electronic supplementary information (ESI) available: further crystal data collection details and figures showing the atomic numbering schemes used. See <http://www.rsc.org/suppdata/dt/b2/b203377c/>

‡ Present address: Department of Applied Chemistry, School of Engineering, University of Tokyo, Hongo, Bunkyo-ku, Tokyo 113-8656, Japan.



Scheme 1

difference = 3.4°). This unsymmetrical feature is partly due to intermolecular π - π interactions of the pyrazolyl and phenyl rings. Several non-bonded interactions with separations of *ca.* 3.5 Å are found [*e.g.* for **2^{Ni}**: C32-C32*: 3.45(1), C32-C103: 3.48(1), C31-C102: 3.524(9), N31-C203: 3.526(9), C13-C22: 3.530(8), N21-C24: 3.546(9), C23-C23: 3.55(1), C13-C204: 3.59(1) Å].

Substitution reactions of the chloro complexes **2** should be performed in a non-coordinating solvent such as CH_2Cl_2 , because donating solvents form adducts of a higher coordination number. For example, reaction of **2** in THF gave the trigonal-bipyramidal THF adducts **2-THF**, which were characterized crystallographically (Table 2 and Fig. S5).⁵ Because the electronic configuration of the resultant adducts is closer to the coordinatively saturated one (18e), they are inert towards further nucleophilic substitution. An analogous THF-adduct, $\text{Tp}^{\text{Ph}}\text{Co-NCS}(\text{THF})$, was reported by Trofimenko *et al.*⁶

Treatment of the chloro complexes **2** and **2'** with silver trifluoromethanesulfonate in acetonitrile readily afforded the corresponding cationic MeCN-coordinated species **1** and **1'**, respectively (Scheme 1). Coordination of three MeCN molecules completes the octahedral coordination sphere as revealed by X-ray crystallography (Fig. 2 and Table 3), which showed C_{3v} -symmetrical core structures for both of the $\text{Tp}^{\text{Ph,Me}}$ (**2**) and Tp^{iPr_2} derivatives (**2'**). The M-N distances are about 2.1 Å and the Co-N distances are slightly longer than the corresponding Ni-N distances due to the larger atomic radius of Co. As for the $\text{Tp}^{\text{Ph,Me}}$ derivatives, the averaged $\text{N}(\text{pz}^{\text{R}})\text{-M-N}(\text{pz}^{\text{R}})$ angles are larger than the averaged $\text{N}(\text{NCMe})\text{-M-N}(\text{NCMe})$ angles by 4°, whereas, for the Tp^{iPr_2} derivatives, the two averaged N-M-N angles are comparable. In addition, deviation of the M-N≡C linkage of the $\text{Tp}^{\text{Ph,Me}}$ derivatives from a linear structure is substantial in contrast to the essentially linear alignment of the Tp^{iPr_2} derivatives. These results suggest that interaction with the π -electrons of the phenyl rings in the $\text{Tp}^{\text{Ph,Me}}$ complexes causes bending of the M-NCMe linkage. Theopold *et al.* reported the analogous $[\text{Tp}^{\text{iPr}_2\text{Me}}\text{Co}(\text{NCMe})_3]^+$ species, which was *in situ* generated by dissolution of $\text{Tp}^{\text{iPr}_2\text{Me}}\text{Co-I}$ in CH_2Cl_2 -MeCN.⁸ Kirchner *et al.* also reported a ruthenium derivative, $[\text{TpRu}(\text{NCMe})_3]\text{PF}_6$, which was found to be less labile than the isoelectronic Cp derivative, $[\text{CpRu}(\text{NCMe})_3]^+$.⁹

The tris-MeCN complexes **1** are so labile as to be stable only in the presence of MeCN. Recrystallization of the nickel

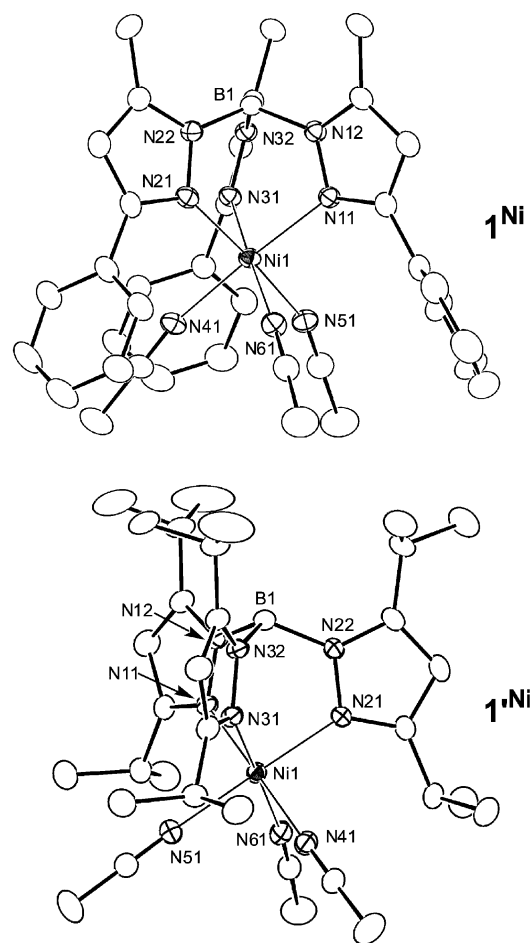


Fig. 2 Molecular structures of the cationic parts of **1^{Ni}** (one of two independent molecules; molecule 1) and **1^{'Ni}** showing 30% thermal ellipsoids.

complex **1^{Ni}** from CH_2Cl_2 -hexane resulted in elimination of one of the three MeCN ligands to give the five-coordinate square-pyramidal bis-MeCN adduct **3** and dissolution of the cobalt complex **1^{Co}** in CH_2Cl_2 resulted in partial decomposition to give the neutral pyrazole-coordinated trifluoromethanesulfonate

Table 2 Selected structural parameters for four- and five-coordinate complexes, $\text{Tp}^{\text{Ph}_3\text{Me}}\text{M}(\text{THF})\text{-Cl}$, $[\text{Tp}^{\text{Ph}_3\text{Me}}\text{M}(\text{L})_n]\text{OTf}$ and $\text{Tp}^{\text{Ph}_3\text{Me}}\text{M}(\text{L})_n\text{-OTf}^e$

Complexes ^b	2 ^c -THF Ni Cl, THF Cl1, O1	3 Ni (NCCCH_3) ₂ N41, N51	4 Co $\text{pz}^{\text{Ph}_3\text{Me}}\text{H}$ N42, O1	5 ^{Ni} Ni { $\text{NCC}(\text{CH}_2)_2\text{CN}$] ₂ N41, N51	7 Co $\text{pz}^{\text{Ph}_3\text{Me}}\text{H}$, $\text{NC}(\text{CH}_2)_2\text{CN}$ N42, N51	8 Ni $\text{NC-C}_6\text{H}_4\text{-CN}$ N41, N51*	9 Ni $\text{NC-C}_6\text{H}_4\text{-CN}$ N41, N51
τ^c	0.46	0.20	0.66	0.35	0.35	0.18	0.14
M-N11	2.052(3)	2.031(2)	2.044(3)	1.999(3)	2.143(4)	2.030(5)	2.025(3)
M-N12	2.052(2)	2.045(3)	2.058(4)	2.054(3)	2.081(3)	2.042(5)	2.035(2)
M-N31	2.094(2)	2.017(2)	2.158(6)	2.000(3)	2.172(4)	2.022(5)	2.024(2)
M-X	2.237(1)	2.041(2)	2.258(3)	2.034(4)	2.082(4)	2.047(5)	2.057(3)
M-Y	2.188(2)	2.070(3)	2.088(4)	2.100(3)	2.108(3)	2.026(5)	2.053(2)
N11-M-N21	93.6(1)	88.06(9)	97.7(1)	87.1(1)	82.3(1)	86.3(2)	88.55(8)
N11-M-N31	91.13(9)	94.06(7)	86.3(1)	95.8(1)	88.6(1)	92.9(2)	92.38(8)
N11-M-X	121.97(8)	161.10(7)	92.9(1)	153.3(1)	173.9(1)	172.7(2)	170.67(7)
N11-M-Y	88.07(8)	90.00(9)	124.9(1)	89.7(1)	89.6(1)	93.5(2)	94.37(9)
N21-M-N31	84.25(9)	90.96(8)	82.5(1)	91.1(1)	95.8(1)	95.9(2)	93.06(6)
N21-M-X	144.18(8)	95.37(9)	93.9(1)	95.8(1)	93.2(1)	91.2(2)	91.93(9)
N21-M-Y	87.47(8)	172.81(7)	136.3(1)	174.1(1)	152.7(1)	162.2(2)	162.49(7)
N31-M-X	97.96(7)	104.43(7)	176.1(2)	110.7(1)	96.1(1)	94.2(2)	96.89(8)
N31-M-Y	171.61(9)	96.09(9)	90.5(1)	110.1(1)	110.1(1)	101.9(2)	104.05(6)
X-M-Y	89.53(6)	84.3(1)	93.1(1)	84.9(1)	92.6(1)	86.7(2)	82.4(1)

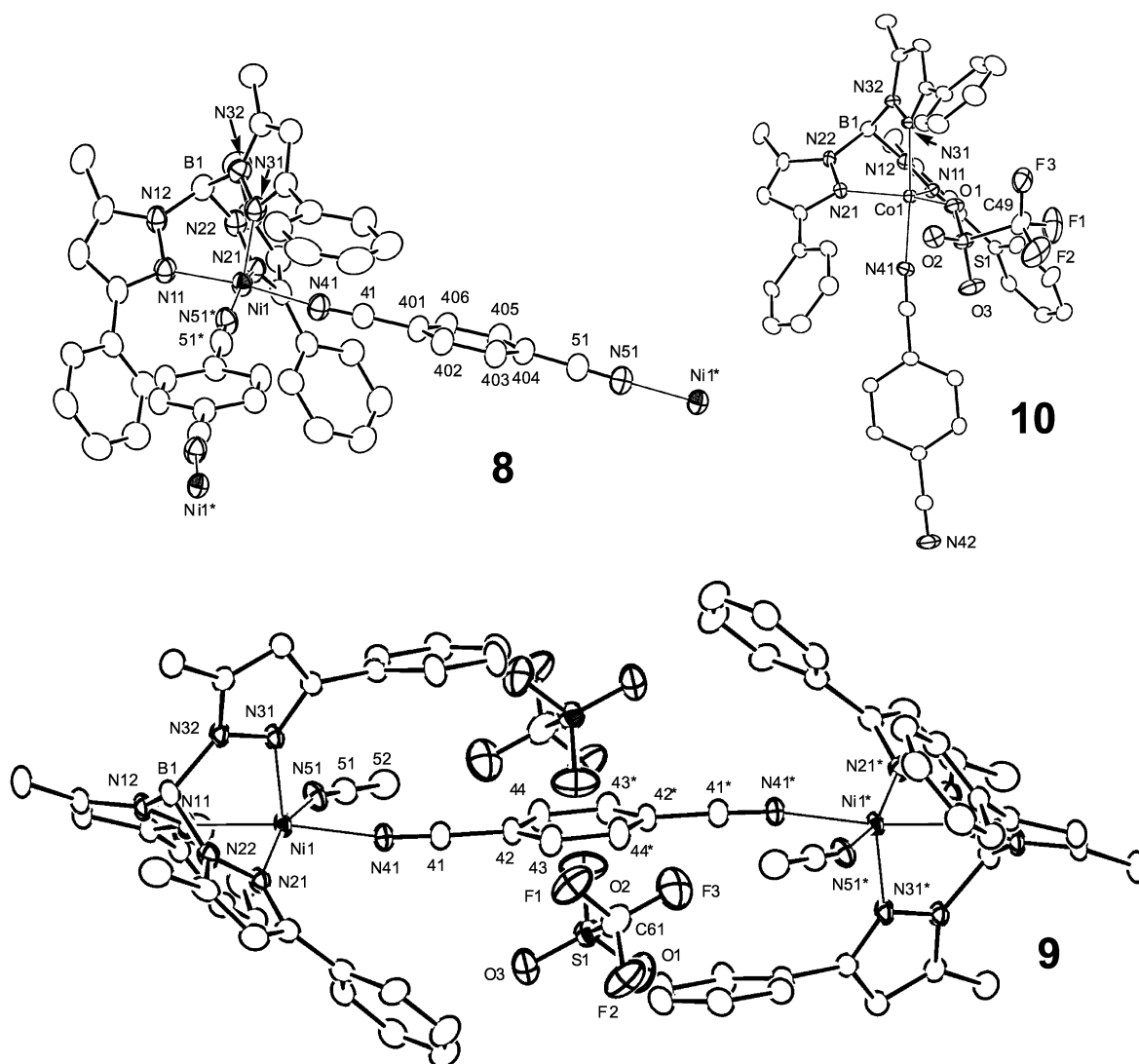
Complexes ^b	11 ^{Ni} Ni (py) ₂	11 ^{Co} Co (py) ₂	12 ^{Ni} Ni α -bipy	12 ^{Co} Co α -bipy	14a Co $\text{Ph}_2\text{P}(\text{CH}_2)_2\text{PPh}_2$	14b ^d Ni $\text{Ph}_2\text{P}(\text{CH}_2)_2\text{PPh}_2$	$\text{Tp}^{\text{Ph}_3\text{Me}}\text{Co-OTf}$ Co —
M	N41, N51	N41, N51	N41, N51	N41, N51	P1, P2	P1A, P2A	P1B, P2B
τ^c	0.58	0.61	0.20	0.05	— ^e	— ^e	— ^e
M-N11	2.049(4)	2.047(5)	2.030(5)	2.040(3)	1.955(3)	1.955(3)	2.018(3)
M-N12	2.049(5)	2.067(5)	2.101(4)	2.053(2)	1.907(5)	1.910(4)	1.928(3)
M-N31	2.131(4)	2.261(4)	2.067(4)	2.072(3)	3.252(4)	3.302(4)	2.020(5)
M-X	2.100(5)	2.064(5)	2.035(5)	2.027(3)	2.2201(9)	2.263(1)	1.963(3)
M-Y	2.022(3)	2.176(5)	2.116(4)	2.063(2)	2.217(2)	2.224(1)	2.232(1)
N11-M-N21	95.7(1)	97.3(2)	84.1(2)	84.0(1)	85.3(1)	84.0(2)	83.7(1)
N11-M-N31	91.1(2)	82.6(2)	97.7(2)	92.7(1)	—	—	93.6(2)
N11-M-X	91.2(2)	158.8(2)	158.8(2)	168.5(1)	166.5(1)	167.2(1)	114.0(1)
N11-M-Y	123.1(2)	86.8(2)	86.8(2)	99.7(1)	100.2(1)	95.9(1)	93.9(1)
N21-M-N31	86.1(2)	89.4(1)	89.4(1)	94.4(1)	—	—	96.5(2)
N21-M-X	90.3(2)	90.3(2)	91.8(2)	94.3(1)	92.4(1)	91.5(1)	113.6(2)
N21-M-Y	141.2(2)	170.9(2)	170.9(2)	165.3(1)	174.16(9)	177.8(1)	175.6(1)
N31-M-X	175.8(2)	89.6(2)	103.0(2)	98.7(1)	—	—	134.0(2)
N31-M-Y	93.4(2)	173.6(2)	93.0(1)	99.6(1)	—	—	—
X-M-Y	88.2(2)	96.8(2)	96.3(2)	79.2(1)	81.76(4)	88.18(4)	88.31(5)

^a Bond lengths in Å and bond angles in deg. ^b N11, N21: the basal or equatorial nitrogen atoms of the $\text{Tp}^{\text{Ph}_3\text{Me}}$ ligand. N31: the axial nitrogen atom of the $\text{Tp}^{\text{Ph}_3\text{Me}}$ ligand. N41, N42, N51: the coordinated nitrogen atoms of the added N-donors. O1: the oxygen atom of the THF ligand or the coordinated oxygen atom of the TIO ligand. P1, P2: the phosphorus atoms of the diphosphines. ^c See text. ^d Two independent molecules. ^e Four-coordinate complexes.

Table 3 Selected structural parameters for [Tp^RM(NCR')₃]OTf **1**, **1'** and **6**^a

Complexes	1 ^{Ni^b}		1 ^{Co^b}		1' ^{Ni}	1' ^{Co}	6
	Molecule 1	Molecule 2	Molecule 1	Molecule 2			
M–N11	2.129(3)	2.135(3)	2.170(4)	2.168(4)	2.082(3)	2.109(2)	2.139(3)
M–N12	2.095(3)	2.088(3)	2.124(4)	2.134(4)	2.076(4)	2.115(2)	2.078(4)
M–N31	2.106(2)	2.103(3)	2.156(3)	2.140(4)	2.079(3)	2.119(2)	2.094(3)
M–N(pz ^R) ^c	2.110	2.109	2.150	2.148	2.079	2.114	2.104
M–N41	2.091(3)	2.125(3)	2.132(5)	2.160(4)	2.119(4)	2.172(3)	2.139(3)
M–N51	2.121(3)	2.125(3)	2.171(4)	2.179(5)	2.127(4)	2.177(3)	2.101(4)
M–N61	2.102(3)	2.099(3)	2.143(4)	2.138(4)	2.120(4)	2.169(3)	2.099(4)
M–N(NCR') ^c	2.105	2.116	2.149	2.159	2.122	2.173	2.113
N–M–N(pz ^R) ^c	88.5	88.5	87.6	87.4	88.9	87.8	89.0
N–M–N(NCR') ^c	84.5	84.0	83.8	83.0	87.3	86.8	83.7
M–N–C(NCR') ^c	166.2	166.2	166.8	167.2	176.3	175.5	178.3

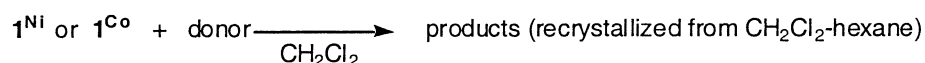
^a Bond lengths in Å and bond angles in deg. ^b Two independent molecules. ^c Averaged values.

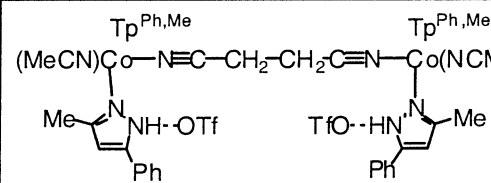
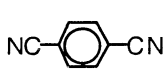
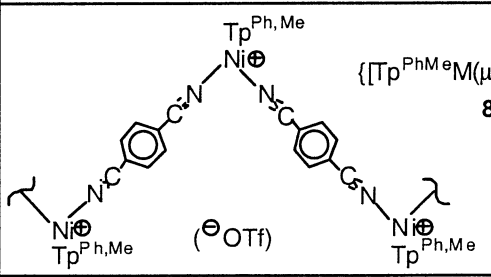
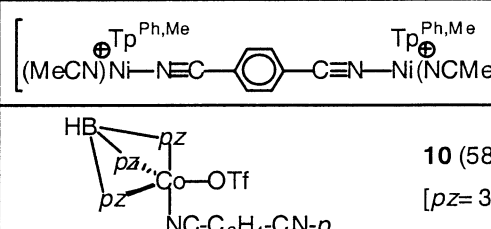
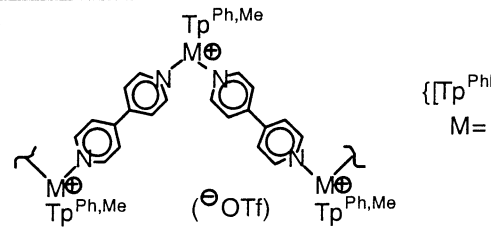
**Fig. 3** Molecular structures of **8–10** (**8**: the cationic part) showing 30% thermal ellipsoids. Labels without atom names are for carbon atoms.

complex **4**.¹⁰ The two products **3** and **4** were characterized by IR and X-ray crystallography (Table 3 and Fig. S6).⁴ It should be noted for **4** that (1) one of the three pyrazolyl groups undergoes borotropic rearrangement¹¹ to give the “reversed” ligand (N31–32, C31–33, and C301–306) and (2) the coordinated pyrazole molecule forms hydrogen bonding interaction with one of the two uncoordinated oxygen atoms of the TfO group [O2···N41: 2.808(3) Å]. Borotropic rearrangement has several precedents.^{1,11} These features of the tris-MeCN complexes **1** suggest

the labile nature of the MeCN ligand, which could be applied for derivative chemistry of Tp^RM species (M = Ni, Co).

As we expected, the cationic tris-MeCN complexes **1** were found to be versatile starting compounds for the [Tp^RM(L)_n]⁺-type cationic complexes *via* treatment with various N- and P-donors (Scheme 2; All reactions were carried out in CH₂Cl₂ and single crystals were obtained by crystallization from CH₂Cl₂–hexane or CH₂Cl₂–toluene–hexane). Because two- or three-dimensional structures are expected to be formed through



donor	M	$\frac{\text{donor}}{\text{M}}$	products ^a
NC-(CH ₂) ₂ -CN	Ni,Co	4	$\left[\text{Tp}^{\text{Ph,Me}} \text{M}^{\oplus} \begin{matrix} \text{NC}-(\text{CH}_2)_2-\text{CN} \\ \text{NC}-(\text{CH}_2)_2-\text{CN} \end{matrix} \right] \ominus \text{OTf}$ M= Ni (5^{Ni} ; 75 %; spy) ^{b,c} Co (5^{Co} ; 51 %; spy) ^c
	Ni	0.8	$\left[(\text{MeCN})_2 \text{Ni}^{\oplus} \text{---} \text{N} \equiv \text{C} \text{---} \text{CH}_2 \text{---} \text{CH}_2 \text{---} \text{C} \equiv \text{N} \text{---} \text{Ni}^{\oplus} (\text{NCMe})_2 \right] (\text{OTf})_2$ 6^b (63 %; oct)
	Co	1	$(\text{MeCN}) \text{Co}^{\oplus} \text{---} \text{N} \equiv \text{C} \text{---} \text{CH}_2 \text{---} \text{CH}_2 \text{---} \text{C} \equiv \text{N} \text{---} \text{Co}^{\oplus} (\text{NCMe})$  7^b (53 %; spy)
	Ni	4	 $\{ [\text{Tp}^{\text{Ph,Me}} \text{M}^{\oplus} (\mu\text{-}p\text{-CN-C}_6\text{H}_4\text{-CN})] \text{OTf} \}$ 8 (85 %; spy) ^b
		1	$\left[(\text{MeCN}) \text{Ni}^{\oplus} \text{---} \text{N} \equiv \text{C} \text{---} \text{C}_6\text{H}_4 \text{---} \text{C} \equiv \text{N} \text{---} \text{Ni}^{\oplus} (\text{NCMe}) \right] (\text{OTf})_2$ 9^b (49 %; spy)
	Co	2	 10 (58 %; spy) ^b [pz= 3-Ph-5-Me-pyrazol-1-yl]
py	Ni,Co	10	$\left[\text{Tp}^{\text{Ph,Me}} \text{M}^{\oplus} \begin{matrix} \text{py} \\ \text{py} \end{matrix} \right] \ominus \text{OTf}$ 11 M= Ni (11^{Ni} ; 81 %; spy) ^b Co (11^{Co} ; 91 %; tbp) ^b
α-bipy	Ni,Co	1	$\left[\text{Tp}^{\text{Ph,Me}} \text{M}^{\oplus} \begin{matrix} \alpha\text{-bipy} \\ \alpha\text{-bipy} \end{matrix} \right] \ominus \text{OTf}$ 12 M= Ni (12^{Ni} ; 86 %; spy) ^b Co (12^{Co} ; 66 %; spy) ^b
p-bipy	Ni,Co	1	 $\{ [\text{Tp}^{\text{Ph,Me}} \text{M}^{\oplus} (\mu\text{-}p\text{-bipy})] \text{OTf} \}$ 13 M= Ni (13^{Ni} ; 86 %; spy) ^b Co (13^{Co} ; 62 %; spy)
Ph ₂ P(CH ₂) _n PPh ₂	Ni	1	$\left[(\kappa^2\text{-Tp}^{\text{Ph,Me}}) \text{Ni}^{\oplus} \begin{matrix} \text{Ph}_2 \\ \text{P} \\ \text{P} \\ \text{Ph}_2 \end{matrix} \right] \ominus \text{OTf}$ 14 n= 2 (14a ; 65 %; spl) ^b n= 3 (14b ; 61 %; py) ^{b,c}
	Co		4 etc.^d

Scheme 2 ^a Coordination geometry of the central metal is shown in parentheses; spy: square-pyramidal; oct: octahedral; tbp: trigonal-bipyramidal; spl: square planar. The hapticity of the Tp^{Ph,Me} ligand is κ³ except for **14** (κ²). ^b Characterized by X-ray crystallography. ^c Recrystallized from CH₂Cl₂-toluene-hexane. ^d See text.

replacement of the MeCN ligands by polyfunctional ligands, reactions with difunctional molecules are also examined.¹² The products except **5^{Co}**¹³ were characterized by X-ray crystallography (Table 2) and the detailed results are included in the ESI.

Complex **5^{Co}** was assigned on the basis of its IR spectrum being very similar to that of the corresponding nickel derivative **5^{Ni}**. The Tp^{Ph,Me} ligand is coordinated as a κ³-ligand except for the diphosphine complexes **14** and the coordination geometry of

the central metal is shown in parentheses (Scheme 2).⁴ The MeCN ligands in **1** were readily replaced by nitriles. Reaction of succinonitrile gave three different types of products **5–7** depending on the donor/M ratio and the central metal. Treatment of **1** with an excess amount of succinonitrile (>2 equivalents) resulted in removal of all three MeCN ligands to afford the mononuclear five-coordinate square-pyramidal 1 : 2-adduct **5**. In principle, 1 : 1 reaction of **1** and a difunctional donor (L) should form an oligomeric or polymeric adduct, $[\text{Tp}^{\text{Ph,Me}}\text{M}(\mu\text{-L})_n(\text{OTf})_n]$. Treatment of **1** with a limited amount of succinonitrile, however, did not produce an expected supra-molecular adduct but the products **6** and **7** arising from incomplete replacement of the MeCN ligands in **1**.¹² The core structure of the nickel complex **6** sitting on a crystallographically imposed centrosymmetric site is essentially the same as that of the starting compound **1**^{Ni}. The cobalt complex **7** contains the pyrazole ligand resulting from partial decomposition of the $\text{Tp}^{\text{Ph,Me}}$ ligand and the N–H moiety also interacts with the triflate anion through a hydrogen bond. Partial decomposition of the Tp^{R} ligand to release pyrazole is frequently observed as was already noted for **4**.¹⁴

Reaction of *p*-dicyanobenzene, a more rigid and slightly strongly donating dinitrile, also afforded three different types of products **8–10**, which showed structural features different from those of the products obtained from succinonitrile. Addition of an excess amount of *p*-dicyanobenzene to the nickel complex **1**^{Ni} resulted in the formation of the polymeric 1 : 1 adduct **8**, and neither 1 : 2-adduct like **5**^{Ni} nor cyclic oligomeric product was formed at all under the present reaction conditions. The infinite zig-zag structure of **8** with the square-pyramidal Ni core was confirmed by X-ray crystallography (Fig. 3 and Table 2). Reduction of the amount of the dinitrile to 1 : 1 ratio caused incomplete replacement of the MeCN ligands in **1**^{Ni} as observed for **6** to give the dinuclear complex **9**. As can be seen from the molecular structure (Fig. 3 and Table 2), the bridging *p*-dicyanobenzene molecule is located in the cavity formed by the phenyl groups of the $\text{Tp}^{\text{Ph,Me}}$ ligands and the triflate anions. In contrast to the nickel system, reaction of the cobalt complex **1**^{Co} produced the neutral TfO-coordinated trigonal-bipyramidal 1 : 1-adduct **10** (Fig. 3) irrespective of the amount of the dinitrile added. Compared to nickel complexes, five-coordinate cobalt complexes, in particular, neutral complexes, prefer a trigonal-bipyramidal geometry.

Pyridine and *o*-bipyridine also produced five-coordinate adducts **11** and **12** but different coordination structures resulted depending on the ligand and the central metal. Reaction of *o*-bipyridine gave the square-pyramidal adducts **12** irrespective of the central metals, whereas that of pyridine afforded the square-pyramidal nickel (**11**^{Ni}) and trigonal-bipyramidal cobalt adducts (**11**^{Co}) as is evident from the τ values (see below).¹⁵

Reaction of *p*-bipyridine gave the polymeric adducts **13** in a manner similar to the 2 : 1 reaction of *p*-dicyanobenzene. Complexes **13**, which were precipitated out of the reaction mixture, were sparingly soluble in CH_2Cl_2 in accord with the infinite zig-zag structure with the square-pyramidal $\text{Tp}^{\text{Ph,Me}}\text{M}$ hinge ($\tau = 0.192$) with the N–M–N(*p*-bipy) angle of 97° as revealed by preliminary X-ray crystallography of **13**^{Ni}.¹³

Reaction of **1**^{Ni} with diphosphines, which would cause a larger crystal field splitting compared to N-donors, produced the diamagnetic, square-planar complexes **14** containing the $\kappa^2\text{-Tp}^{\text{Ph,Me}}$ and κ^2 -diphosphine ligands. The cationic part of complexes **14** are isostructural with the isoelectronic d⁸-rhodium(I) complexes, $(\kappa^2\text{-Tp}^{\text{iPr}_2})\text{Rh}(\kappa^2\text{-diphosphine})$, previously reported by us.^{2c} Reaction of the cobalt derivative **1**^{Co}, however, did not give the corresponding adducts but a mixture containing **4**, the formation of which was indicative of the occurrence of a decomposition process.

As for the structural aspect of the donor adducts, incorporation of two or three donors to the $\text{Tp}^{\text{R}}\text{M}$ fragment leads to a variety of coordination geometries as discussed above.

Coordination of three donor molecules always causes formation of an octahedral structure (**1**, **1'**, **6**), whereas coordination of two donor molecules results in formation of either four- or five-coordinate species depending on the hapticity of the Tp^{R} ligand, κ^2 or κ^3 . All products other than the diphosphine complexes bearing $\kappa^2\text{-Tp}^{\text{Ph,Me}}$ ligand (**14**) adopt a five-coordinate structure between square-pyramidal (spy) and trigonal-bipyramidal geometries (tbp). It is well-known that the two geometries differ little in energy from each other and the distortion from the two ideal geometries can be conveniently indicated in terms of the τ parameter as proposed by Addison *et al.* ($\tau = 0$ for an ideal spy structure; 1 for an ideal tbp structure).¹⁵ The τ values for the complexes which appear in this paper are summarized in Table 2.¹³ In general, neutral complexes (**2**^{Ni}–THF, **2**^{Co}–THF, **4**, **10**) adopt a geometry closer to a trigonal-bipyramidal one (0.46–0.66) irrespective of the central metal. In contrast, as for the cationic complexes, the structures of the nickel complexes (**3**, **5**^{Ni}, **11**^{Ni}, **12**^{Ni}, **13**^{Ni}) are closer to a spy geometry ($\tau = 0.06$ –0.35), whereas the cobalt complexes prefer a tbp geometry (**4**: 0.66; **10**: 0.58; **11**^{Co}: 0.61) unless the geometry is constrained by a chelating ligand with a small bite angle such as *o*-bipy [**12**^{Co}: $\tau = 0.05$; bite angle of *o*-bipy = 79.2(1)°]. The intermediary structure of **7** ($\tau = 0.35$) should be due to steric constraints induced by succinonitrile due to the short span of the two cyano groups, which are bound to the two metal centers.

In summary, the highly labile cationic octahedral tris-MeCN adducts, $[\text{Tp}^{\text{R}}\text{M}(\text{NCMe})_3]\text{OTf}$ **1** and **1'**, have been prepared, fully characterized, and converted to a series of donor adducts *via* MeCN-replacement reactions. The MeCN ligands in **1** and **1'** are so labile that they serve as reactive starting compounds for coupling reactions with substrates with weak nucleophilicity. As we reported recently, the xenophilic complexes with a highly polar metal–metal bond, $\text{Tp}^{\text{iPr}_2}\text{M}–\text{Co}(\text{CO})_4$, were successfully synthesized from **1'**, which was found to be reactive enough to couple with the very weak nucleophile $[\text{Co}(\text{CO})_4]^-$.^{2e} The tris-MeCN complexes **1** and **1'** are potentially useful as a corner block for the architecture of three-dimensional structures and such a possibility is suggested by coupling with difunctional linkers.

Experimental

All manipulations were carried out under an argon atmosphere using standard Schlenk tube techniques. CH_2Cl_2 (P_4O_{10}), MeOH ($\text{Mg}(\text{OMe})_2$), MeCN (CaH_2), THF and hexane (Na–K/benzophenone) were treated with the appropriate drying agents, distilled, and stored under argon. IR spectra (as KBr pellets; reported in cm^{-1}) were obtained on a JASCO FT/IR 5300 spectrometer. NMR spectra were observed on a JEOL Lambda-500 spectrometer (¹H: 500 MHz; ³¹P: 202 MHz). $\text{KTp}^{\text{Ph,Me}}$ was prepared according to the literature procedure.^{6a} Other chemicals were used as received without further purification. Synthetic procedures for the cobalt complexes were essentially the same as those described for the nickel complexes unless otherwise stated.

$\text{Tp}^{\text{Ph,Me}}\text{M}–\text{Cl}$

2^{Ni}: A CH_2Cl_2 solution (20 mL) of $\text{KTp}^{\text{Ph,Me}}$ (1.00 g, 1.90 mmol) was added dropwise to a methanolic solution (2 mL) of $\text{NiCl}_2 \cdot 6\text{H}_2\text{O}$ (455 mg, 1.91 mmol) and the resultant mixture was stirred overnight. After removal of the volatiles under reduced pressure the residue was extracted with CH_2Cl_2 and filtered. Concentration and addition of hexane gave **2**^{Ni} (783 mg, 1.36 mmol, 71 % yield) as purple crystals. IR/ cm^{-1} : 3130 (w), 3059 (w), 2964 (w), 2922 (w, ν_{CH}), 2544 (w, ν_{BH}), 1546 (s, ν_{CN} of $\text{pz}^{\text{Ph,Me}}$). FD–MS: $m/z = 577$ (M^+). Anal. calc. for $\text{C}_{30}\text{H}_{28}\text{N}_6\text{BClNi}$: C, 62.39; H, 4.89; N, 14.55; Cl, 6.14. Found: C, 62.25; H, 4.82; N, 14.61; Cl, 6.11%.

2^{Co} (61% yield; blue crystals). IR/cm⁻¹: 3133 (w), 2961 (w), 2927 (w, ν_{CH}), 2549 (m, ν_{BH}), 1548 (s, ν_{CN} of pz^{PhMe}). FD-MS: m/z = 578 (M⁺). Anal. calc. for C₃₀H₂₈N₆BClCo: C, 62.36; H, 4.88; N, 14.55; Cl, 6.14. Found: C, 62.01; H, 4.58; N, 14.71; Cl, 6.31%.

Recrystallization of **2^{Ni}** and **2^{Co}** from THF gave Tp^{PhMe}-M-Cl(THF) **2^{Ni}-THF** and **2^{Co}-THF**, respectively.

2^{Ni}-THF: yellow crystals; 65% yield. IR/cm⁻¹: 3065 (w), 2974 (m), 2927 (w, ν_{CH}), 2538 (m, ν_{BH}). Anal. calc. for C₃₄H₃₆N₆OBClNi: C, 62.86; H, 5.59; N, 12.94. Found: C, 63.30; H, 5.58; N, 13.32%.

2^{Co}-THF: purple crystals; 46% yield. IR/cm⁻¹: 3127 (w), 3058 (w), 2962 (m), 2919 (w, ν_{CH}), 2549 (m, ν_{BH}). Anal. calc. for C₃₄H₃₆N₆OBClCo: C, 62.48; H, 5.58; N, 12.93; Cl, 5.46. Found: C, 62.64; H, 5.31; N, 13.29; Cl, 5.82%.

[Tp^{PhMe}M(NCMe)₃]OTf

1^{Ni}: Addition of **2^{Ni}** (400 mg, 0.692 mmol) to an MeCN solution (10 mL) of AgOTf (178 mg, 0.692 mmol) caused a color change to green. After the resultant mixture was stirred for 2 h, the precipitates were removed by filtration through a Celite pad. Concentration and crystallization by addition of ether gave **1^{Ni}** (463 mg, 0.569 mmol, 82% yield) as blue crystals. IR/cm⁻¹: 3136 (w), 3063 (m), 2993 (m), 2930 (m, ν_{CH}), 2546 (m, ν_{BH}), 2316 (m), 2290 (m, ν_{CN}). Anal. calc. for C₃₇H₃₇N₉O₃BF₃SNi: C, 52.26; H, 4.86; N, 14.82. Found: C, 52.52; H, 4.59; N, 14.65%.

1^{Co}: 78% yield, brown crystals. IR/cm⁻¹: 3127 (w), 3064 (m), 2931 (w, ν_{CH}), 2544 (m, ν_{BH}), 2314 (m), 2289 (m, ν_{CN}). Anal. calc. for C₃₇H₃₉N₉O₄BF₃SCo (1^{Co}·H₂O): C, 52.26; H, 4.86; N, 14.82. Found: C, 52.52; H, 4.59; N, 14.65%.

[Tp^{iPr}M(NCMe)₃]OTf 1'

1^{Ni,Co} were obtained by essentially the same procedures as described for **1^{Ni,Co}**, starting from Tp^{iPr}M-Cl. Due to partial dissociation of the highly labile MeCN ligands under reduced pressure analytically pure samples could not be obtained.

1^{Ni}: IR/cm⁻¹: 2970 (vs), 2933 (s), 2870 (s, ν_{CH}), 2544 (m, ν_{BH}), 2312 (m), 2285 (m, ν_{CN}).

1^{Co}: IR/cm⁻¹: 2968 (vs), 2931 (s), 2872 (m, ν_{CH}), 2545 (m, ν_{BH}), 2316 (m), 2278 (m, ν_{CN}).

[Tp^{PhMe}Ni(NCMe)₂]OTf 3

Dissolution of **1^{Ni}** (100 mg, 0.123 mmol) in CH₂Cl₂ (10 mL) caused a color change from blue to green. Concentration followed by crystallization from CH₂Cl₂-hexane gave **3** as a green solid (77 mg, 0.099 mmol, 81% yield). IR/cm⁻¹: 3045 (m), 2931 (w, ν_{CH}), 2542 (m, ν_{BH}), 2320 (m), 2292 (m, ν_{CN}). Anal. calc. for C_{38.2}H_{41.2}N₆O₃BF₃SCl_{1.6}[3·(CH₂Cl₂)_{0.5}]: C, 52.27; H, 4.32; N, 13.74; S: 3.93. Found: C, 52.64; H, 4.46; N, 12.69; S, 3.58%.

[HB(pz^{PhMe})₂(pz^{Me,Ph})]Co(H-pz^{PhMe})(OTf) 4

Dissolution of red-purple **1^{Co}** (100 mg, 0.123 mmol) in CH₂Cl₂ (10 mL) gave a blue-violet solution, from which **4** (38 mg, 0.045 mmol, 36%) was isolated as blue-purple crystals after concentration and addition of hexane. IR/cm⁻¹: 3246 (s, ν_{NH}), 3046 (m), 2962 (s, ν_{CH}), 2554 (m, ν_{BH}). Anal. calc. for C₄₁H₃₈N₈O₃-BF₃SCo: C, 58.03; H, 4.39; N, 13.20. Found: C, 57.72; H, 4.52; N, 13.34%.

[Tp^{PhMe}M(L)_n]OTf

MeCN-replacement reactions were carried out in CH₂Cl₂. As a typical example, the synthetic procedure for [Tp^{PhMe}Ni(*o*-bipy)]OTf **12^{Ni}** is shown below. Addition of **1^{Ni}** (112 mg, 0.136 mmol) to a CH₂Cl₂ solution (10 mL) of *o*-bipy (21.5 mg, 0.136 mmol) caused a color change to deep green. Concentration followed by crystallization from CH₂Cl₂-hexane gave **12^{Ni}** as yellow green crystals (100 mg, 0.117 mmol, 86% yield).

IR/cm⁻¹: 3142 (w), 3114 (w), 3079 (m), 2930 (w, ν_{CH}), 2541 (m, ν_{BH}), 1609 (m), 1602 (m, $\nu_{\text{C=N}}$ of *o*-bipy). Anal. calc. for C₄₁H₃₆N₈O₃BF₃SCl₂Ni [12^{Ni}·CH₂Cl₂]: C, 54.10; H, 4.11; N, 12.02. Found: C, 55.48; H, 4.25; N, 12.21%.

The other complexes were prepared by essentially the same methods as described for **12^{Ni}**. The stoichiometry of the donors (donor/1), yield and physical properties of the products were as follows:

5^{Ni}: NC(CH₂)₂CN/1^{Ni} = 4; green crystals (crystallized from CH₂Cl₂-toluene-hexane); 75% yield; IR/cm⁻¹: 3065 (w), 2972 (w), 2934 (m, ν_{CH}), 2551 (m, ν_{BH}), 2291 (ν_{CN}). Anal. calc. for C₃₉H₃₆N₁₀BO₃F₃SNi: C, 55.02; H, 4.26; N, 16.45. Found C, 55.19; H, 4.42; N, 16.10%.

5^{Co}: NC(CH₂)₂CN/1^{Co} = 4; purple crystals (crystallized from CH₂Cl₂-toluene-hexane); 51% yield; IR/cm⁻¹: 3066 (w), 3023 (w), 2975 (w), 2938 (m, ν_{CH}), 2548 (m, ν_{BH}), 2305, 2257 (ν_{CN}). Anal. calc. for C₃₉H₃₆N₁₀BO₃F₃SCo: C, 55.01; H, 4.26; N, 16.45. Found C, 54.51; H, 3.94; N, 16.51%.

6: NC(CH₂)₂CN/1^{Ni} = 0.8; blue crystals (crystallized from CH₂Cl₂-hexane); 63% yield; IR/cm⁻¹: 3118 (w), 3065 (w), 2963 (w), 2934 (m, ν_{CH}), 2547 (m, ν_{BH}), 2314 (m), 2291 (ν_{CN}). Anal. calc. for C_{74.5}H₇₃N₁₈B₂O₆F₆S₂Co₂ [6·(CH₂Cl₂)_{1/2}]: C, 53.61; H, 4.41; N, 15.11. Found C, 53.02; H, 4.40; N, 15.03%.

7: NC(CH₂)₂CN/1^{Co} = 1; purple crystals (crystallized from CH₂Cl₂-hexane); 53% yield; IR/cm⁻¹: 3063 (m), 2990 (w), 2953 (w, ν_{CH}), 2547 (m, ν_{BH}), 2285 (m, ν_{CN}). Anal. calc. for C₈₈H₈₄N₈O₆B₂F₆S₂Cl₄Co₂ [7·(CH₂Cl₂)₂]: C, 54.22; H, 4.34; N, 12.93. Found C, 54.39; H, 4.12; N, 12.90%.

8: *p*-NCC₆H₄CN/1^{Ni} = 4; pale green crystals (crystallized from CH₂Cl₂-hexane); 85% yield; IR/cm⁻¹: 3119 (m), 3099 (w), 3054 (w), 2980 (w), 2961 (w), 2928 (w, ν_{CH}), 2548 (m, ν_{BH}), 2282, 2232 (m, ν_{CN}). Anal. calc. for C_{39.7}H_{33.4}N₈O₃BF₃SCl_{1.4}Ni [8·(CH₂Cl₂)_{0.7}]: C, 54.26; H, 3.83; N, 12.75. Found C, 54.20; H, 3.88; N, 12.74%.

9: *p*-NCC₆H₄CN/1^{Ni} = 1; green crystals (crystallized from CH₂Cl₂-hexane); 49% yield; IR/cm⁻¹: 3097 (w), 3054 (w), 2978 (m), 2931 (w, ν_{CH}), 2548 (m, ν_{BH}), 2371 (m), 2281 (ν_{CN}). Anal. calc. for C₇₄H₆₆N₁₆O₆B₂F₆S₂Ni₂: C, 55.81; H, 4.18; N, 14.07. Found C, 55.27; H, 4.33; N, 14.30%.

10: *p*-NCC₆H₄CN/1^{Co} = 2; green crystals (crystallized from CH₂Cl₂-hexane); 58% yield; IR/cm⁻¹: 3099 (w), 3055 (w), 2927 (m, ν_{CH}), 2547 (m, ν_{BH}), 2278 (m), 2232 (m, ν_{CN}). Anal. calc. for C₄₀H₃₄N₈O₃BF₃SCl₂Co [10·CH₂Cl₂]: C, 53.12; H, 3.79; N, 12.39. Found: C, 53.38; H, 3.96; N, 12.55%.

11^{Ni}: py/1^{Ni} = 10; yellow-green crystals (crystallized from CH₂Cl₂-hexane); 81% yield; IR/cm⁻¹: 3119 (w), 3060 (w), 2927 (w, ν_{CH}), 2540 (m, ν_{BH}), 1639 (m), 1609 (m, $\nu_{\text{C=N}}$). Anal. calc. for C_{41.5}H₃₉N₈O₃BF₃SClNi [11^{Ni}·(CH₂Cl₂)_{0.5}]: C, 55.89; H, 4.41; N, 12.56. Found: C, 55.78; H, 4.18; N, 12.76%.

11^{Co}: py/1^{Co} = 10; red crystals (crystallized from CH₂Cl₂-hexane); 91% yield; IR/cm⁻¹: 3125 (w), 3049 (w), 2961 (w), 2932 (w, ν_{CH}), 2544 (m, ν_{BH}), 1638 (m), 1607 (m, $\nu_{\text{C=N}}$). Anal. calc. for C₄₂H₄₀N₈O₃BF₃SCl₂Co [11^{Co}·CH₂Cl₂]: C, 53.98; H, 4.31; N, 11.99. Found: C, 54.28; H, 4.21; N, 12.25%.

12^{Ni}: *o*-bipy/1^{Ni} = 1; blue-green crystals (crystallized from CH₂Cl₂-hexane); 86% yield; IR/cm⁻¹: 3142 (w), 3114 (w), 3079 (m), 2967 (w), 2930 (w, ν_{CH}), 2541 (m, ν_{BH}), 1609, 1602 (m, $\nu_{\text{C=N}}$). Anal. calc. for C₄₂H₃₈N₈O₃BF₃SCl₂Ni [12^{Ni}·CH₂Cl₂]: C, 54.10; H, 4.11; N, 12.02. Found: C, 54.08; H, 4.25; N, 12.21%.

12^{Co}: *o*-bipy/1^{Co} = 1; brown crystals (crystallized from CH₂Cl₂-hexane); 66% yield; IR/cm⁻¹: 3114 (w), 3064 (m), 2967 (w), 2929 (w, ν_{CH}), 2539 (m, ν_{BH}), 1607 (m, $\nu_{\text{C=N}}$). Anal. calc. for C₄₂H₃₈N₈O₃BF₃SCl₂Co [12^{Co}·CH₂Cl₂]: C, 54.10; H, 4.11; N, 12.02. Found: C, 54.19; H, 4.01; N, 12.41%.

13^{Ni}: *p*-bipy/1^{Ni} = 1; green crystals (crystallized from THF-hexane); 86% yield; IR/cm⁻¹: 3059 (m), 2960 (w), 2929 (m), 2855 (w, ν_{CH}), 2546 (m, ν_{BH}), 1611 (m, $\nu_{\text{C=N}}$). Anal. calc. for C₄₁H₃₆N₈O₃BF₃SNi: C, 58.12; H, 4.28; N, 13.22. Found: C, 57.81; H, 4.31; N, 13.07%.

Table 4 Crystallographic data

Complex	1^{Ni}·MeCN_{0.5}	1^{Ni}·MeCN_{0.5}	1^{Ni}·MeCN_{0.5}	1^{Ni}·MeCN_{0.5}	1^{Ni}·MeCN_{0.5}	2^{Ni}	2^{Ni}	2^{Ni}·THF	2^{Ni}·THF
Formula	C ₃₈ H _{38.5} N _{9.5} O ₃ BF ₃ ⁻	C ₃₈ H _{38.5} N _{9.5} O ₃ BF ₃ ⁻	C ₄₄ H ₇₀ N ₁₄ O ₃ BF ₃ SNi	C ₄₄ H ₆₉ N ₁₄ O ₃ BCoF ₃ S	C ₃₀ H ₂₈ N ₆ BCiNi	C ₃₀ H ₂₈ N ₆ BCiCo	C ₃₄ H ₃₆ N ₆ OBCiNi	C ₃₄ H ₃₆ N ₆ OBCiNi	C ₃₄ H ₃₆ N ₆ BCiCo
Formula weight	834.87	835.08	1001.72	1000.93	577.55	577.77	649.66	649.66	649.88
Crystal system	Triclinic	Triclinic	Triclinic	Triclinic	Monoclinic	Monoclinic	Triclinic	Triclinic	Triclinic
Space group	<i>P</i> $\bar{1}$	<i>P</i> $\bar{1}$	<i>P</i> $\bar{1}$	<i>P</i> $\bar{1}$	<i>P</i> ₂ / <i>n</i>	<i>P</i> ₂ / <i>n</i>	<i>P</i> $\bar{1}$	<i>P</i> $\bar{1}$	<i>P</i> $\bar{1}$
<i>a</i> /Å	12.2099(2)	12.2200(8)	11.9278(16)	11.9437(5)	11.399(3)	11.399(2)	11.085(2)	11.085(2)	11.952(4)
<i>b</i> /Å	30.7377(6)	30.7012(15)	22.495(2)	22.5193(14)	15.991(3)	15.280(4)	12.1868(13)	12.1868(13)	12.119(8)
<i>c</i> /Å	11.3322(2)	11.3355(7)	11.7167(14)	11.6969(4)	15.750(6)	16.261(2)	11.3442(13)	11.3442(13)	11.405(6)
<i>a</i> / $^\circ$	95.5490(10)	95.248(4)	102.376(5)	102.4920(10)	99.724(3)	94.397(12)	93.563(10)	93.563(10)	94.11(5)
β / $^\circ$	103.0680(10)	103.294(2)	113.607(7)	113.435(3)	113.435(3)	94.397(12)	91.331(11)	91.331(11)	91.96(5)
γ / $^\circ$	86.7420(10)	87.084(4)	85.327(6)	85.1750(10)	85.1750(10)	2746.1(9)	78.071(10)	78.071(10)	78.38(5)
<i>V</i> /Å ³	4120.78(13)	4119.5(4)	2813.8(6)	2818.2(2)	2829.7(14)	2746.1(9)	1632.1(3)	1632.1(3)	1613.6(15)
<i>Z</i>	4	4	2	2	4	4	2	2	2
μ /mm ⁻¹	0.583	0.529	0.440	0.399	0.811	0.754	0.713	0.652	0.652
Diffractionmeter	RAXIS IV	RAXIS IV	RAXIS IV	RAXIS IV	RAXIS IV	RAXIS IV	RAXIS IV	RAXIS IV	RAXIS IV
<i>T</i> / $^\circ$ C	-60	-60	-60	-60	-60	-60	-60	-60	-60
No. of variables	936	936	648	648	355	355	400	400	400
<i>R</i> 1 for data	0.0767	0.0920	0.0893	0.0701	0.0946	0.0599	0.0466	0.0466	0.1050
with <i>I</i> > 2 σ (<i>I</i>)	(for 14608 data)	(for 12491 data)	(for 8223 data)	(for 9432 data)	(for 3965 data)	(for 4702 data)	(for 4682 data)	(for 3431 data)	(for 3431 data)
<i>wR</i> 2	0.2425	0.2809	0.2438	0.2131	0.2420	0.1637	0.1537	0.1537	0.2674
	(for all 16357 data)	(for all 16990 data)	(for all 11372 data)	(for all 11642 data)	(for all 4736 data)	(for all 5174 data)	(for all 5747 data)	(for all 5747 data)	(for all 4272 data)
Complex	3	4	5^{Ni}	6-hexane	7-CH₂Cl₂	8-hexane·(CH₂Cl₂)_{2.5}	9	10-CH₂Cl₂	
Formula	C ₃₅ H ₃₄ N ₈ O ₃ BF ₃ SNi	C ₄₁ H ₃₈ N ₈ O ₃ BF ₃ SCo	C ₃₉ H ₃₆ N ₁₀ O ₃ BF ₃ SNi	C ₉₀ H ₈₆ N ₁₈ O ₆ B ₂ F ₆ e ⁻	C ₃₈ H ₃₄ N ₁₈ B ₂ O ₆ F ₆ S ₂ ⁻	C _{47.50} H ₅₁ N ₈ O ₃ BF ₃ ⁻	C ₇₄ H ₆₆ N ₁₆ O ₈ B ₂ F ₆ S ₂ Ni ₂	C ₄₀ H ₃₄ N ₈ O ₃ BF ₃ SCl ₂ Co	
Formula weight	773.28	849.60	851.36	1712.83	1949.13	1171.79	1592.56	904.46	
Crystal system	Triclinic	Monoclinic	Monoclinic	Triclinic	Triclinic	Monoclinic	Triclinic	Orthorhombic	
Space group	<i>P</i> $\bar{1}$	<i>P</i> ₂ / <i>n</i>	<i>P</i> ₂ / <i>c</i>	<i>P</i> $\bar{1}$	<i>P</i> $\bar{1}$	<i>C</i> 2/ <i>c</i>	<i>P</i> $\bar{1}$	<i>Pna</i> 2 ₁	
<i>a</i> /Å	14.0370(19)	15.066(4)	10.5223(5)	12.1603(5)	14.567(2)	20.076(1)	14.2962(5)	23.8843(7)	
<i>b</i> /Å	14.789(3)	14.134(3)	12.9743(8)	15.7044(9)	14.869(2)	16.732(1)	14.8969(8)	17.7515(3)	
<i>c</i> /Å	10.1986(19)	19.942(3)	29.9892(14)	11.5097(6)	12.118(1)	29.573(2)	10.2877(5)		
<i>a</i> / $^\circ$	105.377(15)	99.029(4)	105.678(3)	107.849(7)	102.519(3)	103.579(2)			
β / $^\circ$	66.771(9)	4094.4(14)	100.386(2)	91.345(4)	112.990(5)	109.247(3)			
γ / $^\circ$	1846.8(5)	4	4043.4(4)	75.685(2)	2269.0(4)	9697(1)			
<i>Z</i>	4	4	2	2	4	4	2	2	
μ /mm ⁻¹	0.643	0.533	0.596	0.592	0.605	0.782	0.644	0.646	
Diffractionmeter	RAXIS IV	AFC7R	RAXIS IV	RAXIS IV	RAXIS IV	RAXIS IV	RAXIS IV	RAXIS IV	
<i>T</i> / $^\circ$ C	-60	25	-60	-60	-60	-60	-60	-60	
No. of variables	472	523	526	501	584	519	490	505	
<i>R</i> 1 for data	0.0441	0.0629	0.0592	0.0890	0.0725	0.1100	0.0443	0.0469	
with <i>I</i> > 2 σ (<i>I</i>)	(for 6211 data)	(for 4552 data)	(for 5950 data)	(for 6840 data)	(for 6159 data)	(for 6710 data)	(for 6636 data)	(for 4322 data)	
<i>wR</i> 2	0.1327	0.2136	0.1834	0.2451	0.1816	0.3152	0.1337	0.1369	
	(for all 7608 data)	(for all 7201 data)	(for all 8357 data)	(for all 8434 data)	(for all 9153 data)	(for all 9644 data)	(for all 7653 data)	(for all 4960 data)	

Table 4 (Contd.)

Complex	$11^{\text{Ni}}\text{-CH}_2\text{Cl}_2$	$11^{\text{Co}}\text{-CH}_2\text{Cl}_2$	$12^{\text{Ni}}\text{-CH}_2\text{Cl}_2$	$12^{\text{Co}}\text{-CH}_2\text{Cl}_2$	$14\text{a}\text{-CH}_2\text{Cl}_2\text{-hexane}_{0.5}$	$14\text{b}\text{-(CH}_2\text{Cl}_2)_{0.5}$	$\text{Tp}^{\text{Ph,Me}}\text{Co-OTf-toluene}_{0.5}$
Formula	$\text{C}_{42}\text{H}_{46}\text{BN}_8\text{O}_3\text{F}_3\text{-SCl}_2\text{Ni}$	$\text{C}_{43}\text{H}_{40}\text{N}_6\text{O}_3\text{BF}_3\text{-SCl}_2\text{Co}$	$\text{C}_{49}\text{H}_{38}\text{N}_8\text{O}_3\text{BF}_3\text{-SCl}_2\text{Ni}$	$\text{C}_{49}\text{H}_{38}\text{N}_8\text{O}_3\text{BF}_3\text{-SCl}_2\text{Co}$	$\text{C}_{60}\text{H}_{61}\text{N}_9\text{O}_3\text{BF}_3\text{P}_2\text{-SCl}_2\text{Ni}$	$\text{C}_{58.5}\text{H}_{55}\text{N}_6\text{O}_3\text{BF}_3\text{P}_2\text{S ClNi}$	$\text{C}_{34.5}\text{H}_{32}\text{N}_6\text{O}_3\text{BF}_3\text{SCo}$
Formula weight	934.30	934.30	932.28	932.28	1217.58	1146.05	737.46
Crystal system	Triclinic	Monoclinic	Triclinic	Triclinic	Triclinic	Triclinic	Triclinic
Space group	$P2_1/n$	$P2_1/n$	$P1$	$P1$	$P1$	$P1$	$P1$
$a/\text{\AA}$	12.0847(7)	15.885(4)	12.0690(11)	12.1140(12)	14.009(4)	18.1995(7)	12.0472(18)
$b/\text{\AA}$	18.2862(9)	11.739(3)	15.6895(8)	15.6673(16)	17.556(3)	26.5976(10)	13.7330(15)
$c/\text{\AA}$	10.3024(5)	23.874(5)	11.8660(10)	11.8375(11)	12.878(4)	12.3521(4)	12.0420(19)
a°	94.226(3)	94.49(2)	90.6660(10)	90.428(8)	108.244(13)	102.446(2)	107.381(8)
β°	94.121(4)	94.49(2)	92.674(2)	92.906(8)	83.431(4)	98.393(3)	115.118(3)
γ°	74.8780(10)	4438(2)	103.041(3)	103.388(8)	109.361(9)	72.4820(10)	73.397(8)
$V/\text{\AA}^3$	2188.6(2)	4438(2)	2186.0(3)	2182.4(4)	2837.8(13)	5546.7(3)	1692.1(4)
Z	2	4	2	2	2	2	2
μ/mm^{-1}	0.675	0.615	0.675	0.625	0.592	0.554	0.631
Diffraction	RAXIS IV	AFC7R	RAXIS IV	AFC7R	RAXIS IV	RAXIS IV	RAXIS IV
$T/^\circ\text{C}$	-60	25	25	25	25	25	-60
No. of variables	550	550	553	553	695	1378	438
$R1$ for data with $I > 2\sigma(I)$	0.0993	0.0853	0.0641	0.0540	0.0855	0.0724	0.0625
$wR2$	0.2904	0.2790	0.1820	0.1731	0.2535	0.1905	0.1818
	(for all 8976 data)	(for all 7735 data)	(for all 9002 data)	(for all 7691 data)	(for all 11724 data)	(for all 21687 data)	(for all 6754 data)

13^{Co} : $p\text{-bipy}/1^{\text{Co}} = 1$; brown crystals (crystallized from THF-hexane); 62% yield; IR/cm $^{-1}$: 3059 (w), 2967 (w), 2920 (w), 2855 (w, ν_{CH}), 2543 (m, ν_{BH}), 1611 (s, $\nu_{\text{C=N}}$). Anal. calc. for $\text{C}_{41}\text{H}_{36}\text{N}_8\text{O}_3\text{BF}_3\text{SCo}$: C, 58.10; H, 4.28; N, 13.22. Found: C, 57.74; H, 4.61; N, 13.11%.

14a : $\text{Ph}_2\text{P}(\text{CH}_2)_2\text{PPh}_2/1^{\text{Ni}} = 1$; orange crystals (crystallized from CH_2Cl_2 -hexane); 65% yield; IR/cm $^{-1}$: 3061 (w), 2981 (w, ν_{CH}), 2511 (m, ν_{BH}). $^1\text{H-NMR}$ (CDCl_3): δ_{H} 7.53–6.43 (35H, Ph signals), 6.33 (1H, s, 4-pz-H), 5.88 (2H, s, 4-pz-H), 2.66 (3H, s, 5-pz-Me), 2.57 [2H, t, $^2J_{\text{PH}} = 9$ Hz, $(\text{CH}_2)_2$], 2.52 (6H, s, 5-pz-Me), 1.65 [2H, t, $^2J_{\text{PH}} = 9$ Hz, $(\text{CH}_2)_2$]. $^{31}\text{P-NMR}$ (CDCl_3): δ_{P} 39.70. Anal. calc. for $\text{C}_{58.5}\text{H}_{55}\text{N}_6\text{O}_3\text{BF}_3\text{P}_2\text{SCl}_3$ [$14\text{a}\cdot\text{CH}_2\text{Cl}_2\cdot\text{hexane}_{1.5}$]: C, 57.74; H, 4.56; N, 6.91. Found: C, 58.01; H, 4.60; N, 6.97%.

14b : $\text{Ph}_2\text{P}(\text{CH}_2)_3\text{PPh}_2/1^{\text{Ni}} = 1$; orange crystals (crystallized from CH_2Cl_2 -toluene-hexane); 61% yield; IR/cm $^{-1}$: 3116 (w), 3050 (m), 2924 (m), 2865 (w, ν_{CH}), 2460 (m, ν_{BH}). $^1\text{H-NMR}$ (CDCl_3): δ_{H} 7.70–6.56 (35H, Ph signals), 6.79 (1H, s, 4-pz-H), 5.73 (2H, s, 4-pz-H), 2.84 (3H, s, 5-pz-Me), 2.53 (6H, s, 5-pz-Me), 2.33 (2H, br, CH_2), 2.18 (1H, br, CH_2), 1.39 (2H, br, CH_2), 0.96 (1H, br, CH_2). $^{31}\text{P-NMR}$ (CDCl_3): δ_{P} -8.09. Anal. calc. for $\text{C}_{58.5}\text{H}_{55}\text{N}_6\text{O}_3\text{BF}_3\text{P}_2\text{SCl}_3$ [$14\text{b}\cdot(\text{CH}_2\text{Cl}_2)_{0.5}$]: C, 61.16; H, 4.61; N, 6.74. Found: C, 61.31; H, 4.84; N, 7.33%.

X-Ray crystallography

Crystallographic data are summarized in Table 4. Single crystals of 1^{Ni} , 1^{Co} , $1'^{\text{Ni}}$, $1'^{\text{Co}}$ (MeCN-ether), 2^{Ni} , 2^{Co} , **3**, **4**, **6**, **7**, **8**, **9**, **10**, 11^{Ni} , 11^{Co} , 12^{Ni} , 12^{Co} , **14a** (CH_2Cl_2 -hexane), 5^{Ni} , **14b** (CH_2Cl_2 -toluene-hexane) and 2^{Ni}-THF , 2^{Co}-THF (THF-hexane), and $\text{Tp}^{\text{Ph,Me}}\text{Co-OTf}$ (toluene) were obtained by recrystallization from the solvent systems shown in parentheses and mounted on glass fibers.

Experimental procedures for 1^{Ni} , 1^{Co} , $1'^{\text{Ni}}$, and $1'^{\text{Co}}$ are described below as representative examples, and details for the other complexes are included in the ESI.

Diffraction measurements of 1^{Ni} , 1^{Co} , $1'^{\text{Ni}}$, and $1'^{\text{Co}}$ were made on a Rigaku RAXIS IV imaging plate area detector with Mo- $K\alpha$ radiation ($\lambda = 0.71069$ Å). Indexing was performed from two oscillation images, which were exposed for 5 min. The crystal-to-detector distance was 110 mm. Data collection parameters were as follows: the oscillation range/the number of oscillation images/the exposed time: $2.0^\circ/90/400$ sec/deg (1^{Ni}); $5.0^\circ/36/250$ sec/deg (1^{Co}); $5.0^\circ/36/200$ sec/deg ($1'^{\text{Ni}}$); $5.0^\circ/36/300$ sec/deg ($1'^{\text{Co}}$). Readout was performed with a pixel size of $100 \mu\text{m} \times 100 \mu\text{m}$. Neutral scattering factors were obtained from the standard source. In the reduction of data, Lorentz and polarization corrections and empirical absorption corrections were made. An empirical absorption correction was also made.¹⁶ Crystallographic data and the results of structure refinements are listed in Table 4.

The structural analysis was performed on an IRIS O2 computer using the teXsan structure solving program system obtained from the Rigaku Corp., Tokyo, Japan.¹⁷ Neutral scattering factors were obtained from the standard source.¹⁸

The structures were solved by a combination of the direct methods (SHELXS-86¹⁹ or SAPI91 or SIR92 or MITHRIL90)²⁰ and Fourier synthesis (DIRDIF94).²¹ Least-squares refinements were carried out using SHELXL-97¹⁹ (refined on F^2) linked to teXsan. All the non-hydrogen atoms were refined anisotropically. Unless otherwise stated hydrogen atoms were fixed at the calculated positions. Details of the refinements were as follows. 1^{Ni} , 1^{Co} : Unit cells contained two independent molecules. One of the two TfO anions was found to be disordered. Then isotropic refinements were applied taking into account two components [$F4\text{-}60.59 : 0.41$ (1^{Ni}); $0.53 : 0.47$ (1^{Co})], and highly disordered atoms [C72; F4-6, 4A-6A; O4-6, 6A] were fixed at the final stage of the refinement. The two MeCN solvates (occupancy = 0.5) were refined isotropically, and one of them (N91-C91-C92) was fixed at the final stage of the refine-

ment. $1'^{\text{Ni}}$, $1'^{\text{Co}}$: Two isopropyl groups were found to be disordered. Two components [$1'^{\text{Ni}}$: C28,29 : C28A,29A = 0.595 : 0.405, C38,39 : C38A,39A = 0.590 : 0.410; $1'^{\text{Co}}$: C28,29 : C28A,29A = 0.595 : 0.405, C38,39 : C38A,39A = 0.537 : 0.463] were taken into account for anisotropic refinements and the hydrogen atoms attached to the disordered parts were not included. Methyl hydrogen atoms of the other isopropyl groups were refined using riding models.

CCDC reference numbers 183456–183478.

See <http://www.rsc.org/suppdata/dt/b2/b203377c/> for crystallographic data in CIF or other electronic format.

Acknowledgements

We are grateful to the Ministry of Education, Science, Sports and Culture of the Japanese Government for financial support of this research (Grant-in-Aid for Scientific Research on Priority Areas: 11228201).

References and notes

- S. Trofimenko, *Scorpionates The Coordination Chemistry of Polypyrazolylborate Ligands*, Imperial College Press, London, 1999.
- (a) M. Akita and S. Hikichi, *Bull. Chem. Soc. Jpn.*, 2002, **75**, 1657; (b) N. Kitajima, S. Hikichi, M. Tanaka and Y. Moro-oka, *J. Am. Chem. Soc.*, 1993, **115**, 5496; (c) M. Akita, K. Ohta, Y. Takahashi, S. Hikichi and Y. Moro-oka, *Organometallics*, 1997, **16**, 4121; (d) N. Shirasawa, M. Akita, S. Hikichi and Y. Moro-oka, *Organometallics*, 2001, **20**, 3582; (e) K. Uehara, M. Akita and S. Hikichi, *Organometallics*, 2001, **20**, 5002; (f) S. Hikichi, M. Yoshizawa, Y. Sasakura, H. Komatsuzaki, Y. Moro-oka and M. Akita, *Chem. Eur. J.*, 2001, **7**, 5011; (g) See references cited in 2a–f.
- Abbreviations used in this paper: Tp^{R} : hydrotris(pyrazolyl)borato ligands; Tp^{ipr} : 3,5-diisopropylpyrazolyl derivative; $\text{Tp}^{\text{Ph,Me}}$: 3-phenyl-5-methylpyrazolyl derivative; pz^{R} : pyrazolyl group in Tp^{R} . Compound numbers for the Tp^{ipr} derivatives are indicated with a prime (').
- See ESI.
- The numbering scheme for the non-hydrogen atoms of the cobalt complex is the same as that of the corresponding nickel complex.
- (a) A. L. Rheingold, R. L. Ostrander, B. S. Haggerty and S. Trofimenko, *Inorg. Chem.*, 1994, **33**, 3666; (b) S. Trofimenko, J. C. Calabrese and J. S. Thompson, *Inorg. Chem.*, 1987, **26**, 1507; (c) A. L. Rheingold, L. M. Liable-Sands and S. Trofimenko, *Inorg. Chem.*, 2001, **40**, 6509.
- See discussion in ref. 6c.
- O. M. Reinaud, A. L. Rheingold and K. H. Theopold, *Inorg. Chem.*, 1994, **33**, 2306.
- E. Rüba, W. Simanko, K. Mereiter, R. Schmid and K. Kirchner, *Inorg. Chem.*, 2000, **39**, 382.
- A very small amount of the O-bound trifluoromethanesulfonato complex, $\text{Tp}^{\text{Ph,Me}}\text{Co}-\text{OTf}$, was occasionally isolated from the mixture but was characterized only by IR and X-ray crystallography.⁴ IR ν_{BH} 2547 cm^{-1} .
- A. Albinarti, M. Bovens, H. Rügger and L. M. Venanzi, *Inorg. Chem.*, 1997, **36**, 5991 and references cited therein.
- (a) Examples of formation of three-dimensional structures using dinitrile: S. Mann, G. Huttner, L. Zsolnai and K. Heinze, *Angew. Chem., Int. Ed. Engl.*, 1996, **36**, 2808; (b) S. Mann, G. Huttner, L. Zsolnai, K. Heinze, V. Jacob, B. Antelmann, A. Driess and B. Schiemenz, *Z. Naturforsch., Teil B*, 2000, **55**, 638; (c) L. Carlucci, G. Ciani, P. Macchi, D. M. Proserpio and S. Rizzato, *Chem. Eur. J.*, 1999, **5**, 237.
- The structural report of 13^{Ni} is not included in this paper because of the low convergence, which was attributed to the highly disordered TfO anion, but the structure of the cationic part was refined satisfactorily. The current *R*1 value (TfO not included in the refinement) is 0.14. Because the cell parameters for 13^{Co} , crystals of which were of lower quality, were very similar to those of 13^{Ni} , these two species should be isostructural. Crystallographic data for 13^{Ni} : $a = 14.336(2)$, $b = 15.717(2)$, $c = 10.4037(9)$ Å, $\alpha = 97.462(5)$, $\beta = 101.952(6)$, $\gamma = 106.348(2)^\circ$, $V = 2155.9(4)$ Å³.
- See also, for example, (a) S. Hikichi, T. Ogihara, K. Fujisawa, N. Kitajima, M. Akita and Y. Moro-oka, *Inorg. Chem.*, 1997, **36**, 4539; (b) M. Kosugi, S. Hikichi, M. Akita and Y. Moro-oka, *Inorg. Chem.*, 1999, **38**, 2567.
- (a) A. W. Addison, T. N. Rao, J. Reedijk, J. van Rijn and G. C. Verschoor, *J. Chem. Soc., Dalton Trans.*, 1984, 1349. See also; (b) S. Alvarez and M. Llunell, *J. Chem. Soc., Dalton Trans.*, 2000, 3288.
- T. Higashi, Program for absorption correction, Rigaku Corp., Tokyo, Japan, 1995.
- teXsan, Crystal Structure Analysis Package, v. 1.11, Rigaku Corp., Tokyo, Japan, 2000.
- D. T. Cromer and J. T. Waber, *International Tables for X-Ray Crystallography*, Kynoch Press, Birmingham, 1975, vol. 4.
- (a) G. M. Sheldrick, SHELXS-86: Program for crystal structure determination, University of Göttingen, Göttingen, Germany, 1986; (b) G. M. Sheldrick, SHELXL-97: Program for crystal structure refinement, University of Göttingen, Göttingen, Germany, 1997.
- (a) SAPI91: H.-F. Fan, Structure Analysis Programs with Intelligent Control, Rigaku Corp., Tokyo, Japan, 1991; (b) SIR92: A. Altomare, M. C. Burla, M. Camalli, M. Cascarano, C. Giacovazzo, A. Guagliardi and G. Polidori, *J. Appl. Crystallogr.*, 1994, **27**, 435; (c) MITHRIL90: C. J. Gilmore, MITHRIL – an integrated direct methods computer program, University of Glasgow, Glasgow, UK, 1990.
- P. T. Beurskens, G. Admiraal, G. Beurskens, W. P. Bosman, S. Garcia-Granda, R. O. Gould, J. M. M. Smits, and C. Smykalla, The DIRDIF program system, Technical Report of the Crystallography Laboratory, University of Nijmegen, Nijmegen, The Netherlands, 1992.